COUPLING OF MARS LOWER AND UPPER ATMOSPHERE REVISITED: IMPACTS OF GRAVITY WAVE MOMENTUM DEPOSITION ON UPPER ATMOSPHERE STRUCTURE

S. W. Bougher and T. McDunn, AOSS Department, University of Michigan, Ann Arbor, MI, USA (bougher@umich.edu); **J. Murphy and M. Chizek**, Astronomy Department, New Mexico State University, Las Cruces, NM, USA; **A. Kleinböhl**, Jet Propulsion Laboratory, Pasadena, CA, USA.

Introduction:

The Mars thermosphere (~100-200 km) is an intermediate atmospheric region strongly impacted by coupling below with the lower atmosphere (e.g. seasonal inflation/contraction, gravity waves, planetary waves and tides, dust storms) and coupling above with the Sun (solar soft X-ray, EUV, UV and near IR fluxes, and solar wind particles) [e.g. Bougher et al., 2008 review]. A wide assortment of modeling studies have been conducted in recent years to investigate the role of upward propagating planetary and tidal waves upon the upper atmosphere structure and dynamics [e.g. Forbes et al., 2002; Bell et al., 2007; Gonzalez-Galindo et al., 2009a,b; Moudden and Forbes, 2010]. It is evident that the lower-middle (~0-90 km) atmosphere thermal and wind structure regulates this upward propagation of planetary waves and tides, thereby modifying the upper atmosphere thermal and wind structure as well. One prominent manifestation of this coupling is the observed winter polar warming at lower thermospheric altitudes [e.g. Keating et al., 2003; Bougher et al.,2006; Gonzalez-Galindo et al., 2009b].

Recent temperature datasets spanning MY28-29 are now available for the lower-middle atmosphere of Mars (up to ~90 km) from the Mars Reconnaissance Orbiter (MRO) Mars Climate Sounder (MCS) experiment [e.g. *Kleinböhl et al,* 2009; McCleese et al. 2008; 2010]. These datasets are ideal to constrain atmosphere thermal structure as a function of season, and specifically to investigate the changing atmospheric patterns of winter polar warming [McDunn et al., 2011]. These datasets also provide for the first time detailed constraints for General Circulation Models (GCMs) that couple the lower and upper atmospheres of Mars.

Numerical studies using the coupled MGCM-MTGCM framework [e.g. Bougher et al., 2004; 2006; 2008; 2009] have recently utilized these MCS datasets to constrain lower-middle atmosphere temperatures (up to 90 km). In so doing, it has become clear that gravity wave (GW) momentum deposition is missing from the numerical formulation. A Palmer-type GW momentum deposition scheme (tuned for Martian conditions) has been added recently to the Ames MGCM, thereby enabling the observed atmosphere temperature structure (e.g. winter polar warming features) to be more accurately simulated throughout the Martian year. The associated impacts of these improved Ames MGCM temperature and wind fields upon the MTGCM thermospheric structure and dynamics are investigated in this presentation. The Ls = 270 solstice season is initially selected for study.

New MRO/MCS Atmosphere Datasets:

The Mars Climate Sounder (MCS) is a passive infrared radiometer onboard NASA's Mars Reconnaissance Orbiter (MRO). MRO entered its science-phase, near-polar, sun-synchronous orbit on September 24, 2006 (L_s 111°, MY28). The sun-synchronicity of MRO's orbit determines that MCS repeatedly observes the atmosphere at two local times as the planet rotates underneath the orbiting spacecraft. In other words, each time the spacecraft passes over the dayside, it does so at approximately 3PM (except near the poles, where where the LST varies rapidly as the spacecraft passes over the pole itself) and each time it passes over the nightside it does so at approximately 3 AM. Meanwhile the planet spins beneath, effectively varying the longitude observed on each pass. The near-polar trajectory of the orbit combined with the orbital period allows MCS to map nearly all latitudes during each pass. In its 4+ years of operations, MCS has accumulated nearly 2 million profiles [*McCleese et al* 2008; 2010].

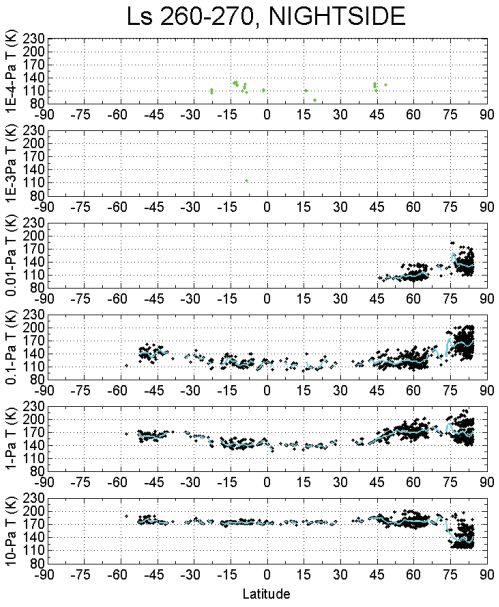

Figure 1. MRO/MCS temperatures (Ls = 260-270 on the nightside) arranged as a function of latitude at distinct pressure levels from 10-Pa to 0.01 Pa (~30 to 85 km). Cyan line indicates averages in 0.5-degree latitude bins. From McDunn et al. (2011).

MCS measures thermally emitted radiation in both limb and on-planet geometries. From these, vertical profiles of pressure and temperature are retrieved using a

modified Chahine method and the Curtis-Godson approximation [*Kleinböhl et al,* 2009]. Nominally, MCS retrieves temperature up to ~80-90 km. This depends somewhat on pointing (i.e. which part of the atmosphere is covered by the MCS detector array) and on temperature at high altitudes (corresponding to signal-to-noise). However, during MY 28 (Ls = 181-258), the lowest topsides occurred near 50 km at southern winter latitudes and the highest topsides occurred near 90 km at southern summer latitudes. This 1-time restriction was entirely due to pointing as the MCS instrument was not tracking the limb during this period. The depth to which retrievals are possible (e.g. limb only) is mostly dependent upon atmospheric opacity. However, in the latest version of the retrieval, on-planet views can be simultaneously retrieved with limb measurements. If an on-planet view is available, the temperature profile typically reaches down to the surface. The vertical resolution of the retrievals is ~5 km with uncertainties on the order of 2 K [*Kleinböhl et al,* 2009]. Figure 1 illustrates MCS temperature retrievals as a function of latitude at selected pressure levels for MY28. Notice that middle atmosphere winter polar warming first becomes visible at about the 1.0 Pa pressure level; it becomes quite substantial (~60 K) at 0.1-Pa.

Coupled MGCM-MTGCM Framework:

The Mars Thermospheric General Circulation Model (MTGCM) is a finite difference primitive equation model that self-consistently solves for time-dependent neutral temperatures, neutral-ion densities, and three component neutral winds over the Mars globe [see details in Bougher et al. 2004, 2006, 2008; 2009; Bell et al. 2007]. Briefly, the modern MTGCM code contains prognostic equations for the major neutral species (CO_2, CO, N_2, and O), selected minor neutral species (Ar, NO, $N(^4S)$, O_2), and several photo-chemically produced ions (e.g. O_2^+ , CO_2^+ , O^+, and NO^+). All fields are calculated on 33 pressure levels above p=1.32 μbar, corresponding to altitudes from roughly ~70 to 250 km, with a 5° resolution in latitude/longitude. The vertical coordinate is log pressure, with a vertical spacing of 0.5 scale heights. A fast non-Local Thermodynamic Equilibrium (NLTE) 15-micron cooling scheme is implemented in the MTGCM, along with corresponding near-IR heating rates [Bougher et al. 2006]; these inputs are based upon the 1-D NLTE model calculations of Lopez-Valverde et al. [1998].

The MTGCM is driven from below by the NASA Ames Mars MGCM code [e.g. Haberle et al. 1999; 2003] at the 1.32-μbar level (near 60-80 km). This coupling allows both the migrating and non-migrating tides to cross the MTGCM lower boundary and the effects of the expansion and contraction of the Mars lower atmosphere to extend to the thermosphere. The entire atmospheric response to simulated dust storms can also be calculated using these coupled models. Key prognostic variables are passed upward from the MGCM to the MTGCM at the 1.32-μbar level at every MTGCM grid point: temperatures, zonal and meridional winds, and geopotential heights. These two climate models are each run with a 2-minute time step, with the MGCM exchanging fields with the MTGCM at this frequency. This MGCM-MTGCM detailed coupling is crucial to conducting realistic simulations of the Mars upper atmosphere structure and dynamics [e.g. Bell et al. 2007].

GW Momentum Deposition Scheme:

The GW parameterization scheme of Palmer et al [1986] has recently been implemented into the NASA Ames MGCM [Hollingsworth and Kahre, 2010; Kahre et al., 2008]. The scheme accounts for the vertical propagation of topographically forced buoyancy wave activity. This scheme has previously been one of several schemes used in Mars GCMs [Collins et al., 1997; Forget et al., 1999]. The surface forced waves, with an amplitude dependent upon the local topographic variance, near-surface wind speed, and near surface atmospheric stability, propagate vertically. Wave momentum deposition within a model layer, resulting in acceleration of the zonal wind within that layer toward a speed of zero m/sec, occurs due to both wave saturation and critical level processes. Saturation arises when the thermodynamic conditions within a layer permit some, but not all, of the wave energy to propagate upward through the layer. The portion of wave energy not permitted to traverse the layer results in an acceleration of the flow within that layer. Complete wave momentum deposition occurs in those layers where upward propagating wave energy meets a zonal wind vector opposite to the direction of the surface wind which forced the wave activity. Since atmospheric density declines with increasing height while the wave's momentum flux remains constant, the magnitude of zonal wind acceleration can be of quite large magnitude if wave activity penetrates to those altitudes.

MGCM simulations to date indicate that the GW effects accounted for with the GW scheme result in reduced winter hemisphere eastward zonal jet wind speeds. These decelerations are accompanied by warmed winter polar temperatures as expected, and as has been demonstrated elsewhere [Collins et al., 1997]. Sensitivity studies have been conducted to determine proper settings for a tunable parameter included in the calculation of the surface wave forcing magnitude. These sensitivity studies involve annual simulations forced with observed MGS TES year 1 dust opacity values. Model results are assessed via comparison with MCS-derived atmospheric temperatures (at polar latitudes primarily) and with Mars atmosphere gravity wave amplitude derivations of Creasey et al [2006] and Fritts et al [2006], as well as Creasey's technique applied to other data sets (e.g. MCS profiles) .

Upper Atmosphere Modeling Results:

Coupled MGCM-MTGCM simulations were conducted for Ls = 270 and F10.7 = 130 conditions, making use of dust opacities from TES Year #1. In addition, two cases were run: (a) without GW momentum deposition, but using Rayleigh friction at the top of the MGCM, and (b) with GW momentum deposition, now neglecting Rayleigh friction. Figures 2a,b (no GW) and 3a,b (with GW) are presented to compare zonal mean temperatures and meridional winds; these are some key impacts of GW momentum deposition on the upper atmosphere structure.

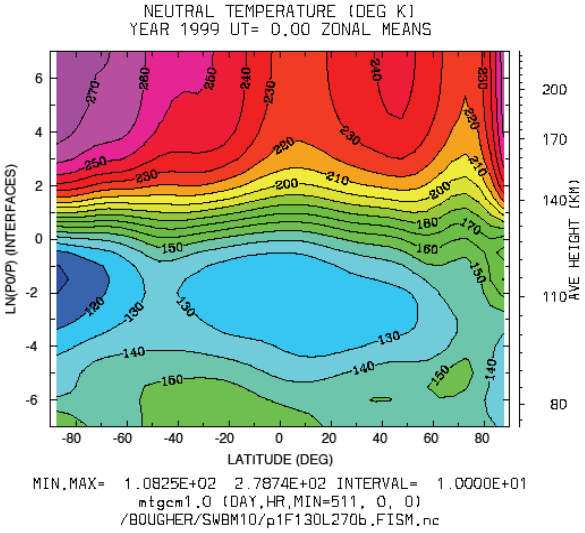

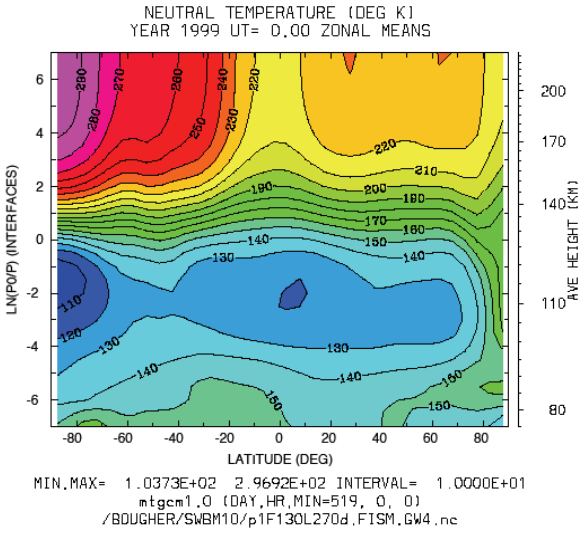

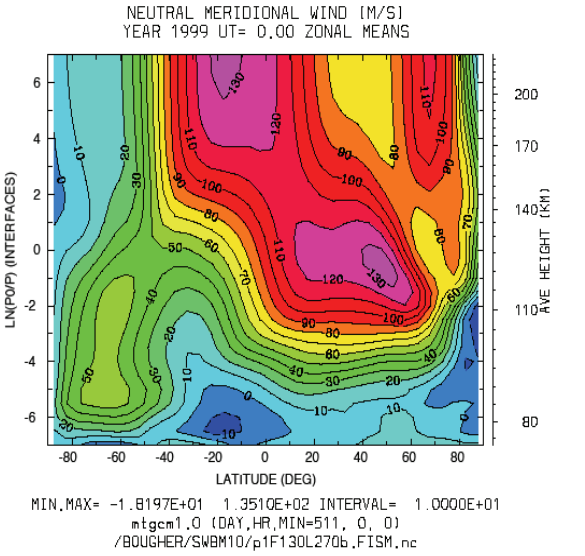

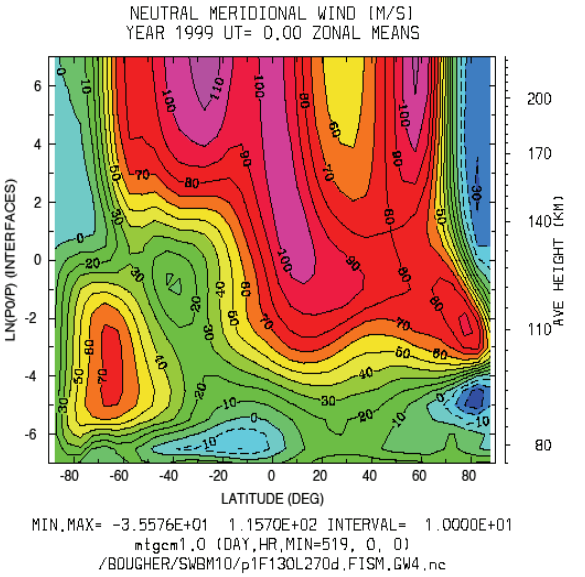

Figures 2a,b: Zonal mean neutral temperatures and meridional winds (~70 to 220 km); Coupled MGCM-MTGCM simulation for no GW forcing; Rayleigh friction is implemented in the MGCM.

Figures 3a,b: Zonal mean neutral temperatures and meridional winds (~70 to 220 km); Coupled MGCM-MTGCM simulation including GW forcing; no Raleigh friction is implemented at the model top.

Conclusions and Future Plans:

These few coupled MGCM-MTGCM simulations suggest that proper implementation of GW momentum deposition in the Mars lower-middle atmosphere has at least three effects: (a) to slow the zonal flow in the winter polar region and to enhance the meridional flow, thereby warming temperatures near the same winter pole toward observed values (~30-85 km); (b) to modify the thermal and wind structure near the base of the thermosphere (80-110 km); and (c) to modify the zonal and meridional winds in the thermosphere, thereby reducing the magnitude of the winter polar warming from that simulated previously [Bougher et al., 2006] toward observed values.

Future work involves the incorporation of this same GW momentum deposition scheme into the existing Mars GITM code (0-250 km) that is presently being validated at the U. of Michigan [e.g. Pawlowski et al., 2010; Bougher et al., 2011].

References:

Bell, J.M., S.W. Bougher, and J.R. Murphy. 2007, JGR, 112, doi:10.1029/2006JE002856.

Bougher, S.W., S. Engel, D.P. Hinson, and J.R. Murphy., 2004, JGR, 109, doi: 10.1029/2003JE002154.

Bougher, S.W., J.M. Bell, J.R. Murphy, P.G. Withers, and M. López-Valverde. 2006, Geophys. Res. Lett., 33, doi: 10.1029/2005GL024059.

Bougher, S.W., P.-L. Blelly, M. Combi, J.L. Fox, I. Mueller-Wodarg, A. Ridley, and R.G. Roble. 2008, Sp. Sci. Rev., 139, doi: 10.1007/s11214-008-9401-9.

Bougher, S.W., T.M. McDunn, K.A. Zoldak, and J.M. Forbes, 2009, GRL, 36, L05201, doi:10.1029/2008GL036376.

Bougher, S. W., A. Ridley, D. Pawlowski, J. Murphy, S. Nelli, 2011. Abstract, Mars Atmosphere; Modeling and Observations Workshop, Paris, February 8-11, 2011

Collins, M., S. Lewis, and P. Read, 1997, Adv. Space Res., 19, 1245-1254.

Creasey, J, J. Forbes, and D. Hinson, 2006, GRL, 33, L01803, doi:10.1029/2005GL024037.

Forbes, J. M., A. F. C. Bridger, S. W. Bougher, M. E. Hagan, J. L. Hollingsworth, G. M. Keating, and J. Murphy, 2002), J. Geophys. Res., 107(E11), 5113, doi:10.1029/2001JE001582.

Forget, F., F. Hourdin, R. Fournier, C. Hourdin, O. Talagrand, M. Collins, S. Lewis,, P. Read, and J.-P. Huot, 1999, J. Geophys. Res., 104, 24155-24176.

Fritts, D., L. Wang, and R.Tolson, 2006, J. Geophys. Res., 111, A12304, doi:10.1029/2006JA011897.

Gonz´alez-Galindo, F., Forget, F., L´opez-Valverde, M. A., Angelats i Coll, M., & Millour, E. 2009a, Journal of Geophysical Research (Planets), 114, 4001.

Gonz´alez-Galindo, F., Forget, F., L´opez-Valverde, M. A. & Angelats i Coll, M. 2009b, Journal of Geophysical Research (Planets), 114, 8004.

Haberle, R.M., Joshi, M.M., Murphy, J.R., Barnes, J.R., Schofield, J.T., Wilson, G., López-Valverde, M., Hollingsworth, J.L., Bridger, A.F.C., Schaeffer, 1999. JGR, 104, doi: 10.1029/1998JE900040.

Haberle, R. M., J. L. Hollingsworth, A. Colaprete, A. F. C. Bridger, C. P. McKay, J. R. Murphy, J. Schaeffer, and R. Freedman, 2003, *Published Conference Abstract, International Workshop: Mars Atmosphere Modelling and Observations*, Granada, Spain, January 13-15, 2003.

Hollingsworth, J.L, and M. Kahre, 2010, GRL, 37, Lsss02, doi:10.1029/2010GL044262

Kahre, M.A., J. Hollingsworth, R. Haberle, and J. Murphy, 2008, ICARUS, 195, 576-597, doi:10.1016/j.icarus.2008.01.023

Keating, G. M., et al. (2003), Published Abstract, Mars Atmosphere Modelling and Observations, Cent. Natl. d'Etudes Spatiales, Granada, Spain, 13– 15 Jan. 2003.

Kleinböhl A. et al., 2009, *J. Geophys. Res., 114,* doi:10.1029/2009JE003358.

López-Valverde, M.A., D.P. Edwards, M. López-Puertas, and C. Roldán. 1998, , JGR, 103, 16,799-16,812, 1998.

McCleese D. et al., 2008, *Nature,* doi: 10.1038/ngeo332.

McCleese D. et al., 2010, submitted, *J. Geophys. Res.*

McDunn, T.,S. Bougher, A. Kleinboehl,, F. Forget, 2011, abstract, Mars Atmosphere; Modeling and Observations Workshop, Paris, February 8-11, 2011.

Moudden, Y. and J. M. Forbes, 2010, JGR, 115, E09005, doi:10.1029/2009JE003542.

Palmer, T., J. Shutts, and R. Swinbank, 1986, Q. Journ. Royal Met Society, 112, 1001-1039.

Pawlowski, D., S. W. Bougher, and A. Ridley, 2010. 38th COSPAR Assembly, Abstract # 6194, Bremen, Germany. July (2010);